

Absolute measurements of optical oscillator strengths of noble-gas resonance lines

N. D. Gibson* and J. S. Risley

North Carolina State University, Raleigh, North Carolina 27695

(Received 19 April 1995)

We have remeasured the optical oscillator strengths of eight noble-gas resonance lines in the vacuum-ultraviolet region. The measurements use a 900-eV collimated electron beam to excite the atoms, and the transmission of the emitted radiation is measured as a function of the gas density. In the method of self-absorption used here, the measured oscillator strengths are proportional to the distance between the electron beam and the fixed aperture of the spectrometer-detector system. We investigated and eliminated a possible systematic effect in the determination of the absorption length due to deflections of the electron beam. These measurements are performed at higher energies than our previous experiments at 100 eV in order to keep the electron-beam path better defined and aligned with the electron-gun apertures. The measured absolute oscillator strengths are He I (58.4 nm), 0.2700 ± 0.0076 (2.8%); He I (53.7 nm), 0.0737 ± 0.0023 (3.1%); Ne I (74.4 nm), 0.01095 ± 0.00032 (2.9%); Ne I (73.6 nm), 0.1432 ± 0.0038 (2.6%); Ar I (106.7 nm), 0.0580 ± 0.0017 (2.9%); Ar I (104.8 nm), 0.2214 ± 0.0068 (3.1%); Kr I (123.6 nm), 0.1775 ± 0.0050 (2.8%); and Kr I (116.5 nm), 0.1416 ± 0.0041 (2.9%).

PACS number(s): 32.70.Cs

I. INTRODUCTION

We report the results of our latest measurements of optical oscillator strengths of noble-gas atoms. These measurements include transitions from the ground state to the first and second excited states of helium, argon, neon, and krypton. This work is a continuation and a refinement of our previous study of optical oscillator strengths [1]. These more accurate oscillator strengths are measured to even greater precision than our previous results and therefore constitute better benchmarks for theoretical calculations and more precise data for analysis of phenomena in plasma physics, astrophysics, and the atmospheric sciences.

The atomic-absorption oscillator strengths reported here are measured using the method of self-absorption of resonance radiation. A collimated beam of electrons passing through a gas cell collisionally excites the gas atoms, which then emit resonance radiation. A spectrometer and photomultiplier tube are used to collect radiation emitted at right angles to the electron beam. Some of the resonant radiation is reabsorbed by gas atoms in the cell. The transmission $T_R(n)$ of radiation is measured as a function of the number density n of the gas. The absorption oscillator strengths are determined by analyzing the transmission functions.

Throughout this work the authors will only summarize the techniques and equipment used and explain in detail all differences between this study and our previous experiments. The interested reader is referred to Ref. [1] for further details.

II. SELF-ABSORPTION MEASUREMENTS

The principle of self-absorption of resonance radiation has been described in detail in Ref. [1]. A summary is pre-

sented below. The transmission function $T_R(a_0x)$ is defined as the ratio of the total intensity of a resonance line at a distance x from the source to the total initial intensity at $x=0$. The quantity a_0 is given by

$$a_0 = \frac{e^2}{4\pi\epsilon_0 mc} \left[\frac{\pi M}{2kT} \right]^2 \lambda_0 f n, \quad (1)$$

where e is the electron charge, m is the mass of the electron, ϵ_0 is the vacuum permittivity, M is the mass of the noble-gas atom, T is the temperature of the gas cell, λ_0 is the wavelength of the resonant transition, n is the number density of the gas, and f is the absorption oscillator strength of the transition. The transmission function can be written

$$T_R(a_0x) = \frac{I(x)}{I(0)} = \frac{\int_0^\infty I(\nu, 0) e^{-a(\nu)x} d\nu}{\int_0^\infty I(\nu, 0) d\nu}. \quad (2)$$

Doppler broadening is the dominant factor governing our line shape and hence the absorption and emission profiles are the same. In this situation, the transmission function in Eq. (2) can be expanded in a power series,

$$T_R(a_0x) = \sum_{n=0}^{\infty} \frac{(-a_0x)^n}{n! \sqrt{n+1}}. \quad (3)$$

The first 18 terms in this series produce an accuracy of 1 part in 10^{10} and the transmission function is fitted to the data using this series expansion.

III. APPARATUS

The experimental apparatus is mainly composed of an electron beam, a gas cell, and a Seya-Namioka vacuum monochromator with a photomultiplier tube detector [1-4]. The spectrometer-detector system was well characterized for our previous studies and was not modified for the present experiments. There were three main improvements in the rest

*Present address: Physics Dept., 1150 University Ave., University of Wisconsin, Madison, WI 53706.

of the apparatus that helped us to refine our measurements. The transmission distance between the electron-atom source and the spectrometer entrance slit was more carefully controlled, the gas temperature was better stabilized as well as more precisely determined for the Ar I (106.7 nm) and Ar I (104.8 nm) measurements, and the reemission shielding was greatly improved.

One way the transmission distance was better defined is that the electron gun was run with an energy of 900 eV instead of 100 eV as in our previous measurements with He, Ne, and Kr or 60 eV as for our previous work with Ar. The higher-energy beam is less susceptible to electrostatic and magnetic deflections which would change the electron-atom source to spectrometer entrance slit distance. These deflections could be either permanent due to unchanging magnetic fields or transitory such as would be produced by slowly varying voltages due to surface charges. In addition to producing a stiffer electron beam, the higher electron beam energy produces a greater beam current and increases the quality of the transmission data. Furthermore, the 900-eV electron beam tends to be better focused and thus helps to define the electron-atom source to spectrometer entrance slit distance more precisely.

Additionally, potentially deflecting magnetic fields were reduced inside the collision chamber. Possible evidence of magnetic-field deflections of the electron beam were discovered after a 90° rotation of the electron-atom source and the collision chamber. Two possible causes of these deflections were discovered and corrected. The filament wires carry approximately 3 A when the electron source is producing 2.0×10^{-4} A of electron-beam current. Sections of the wires were previously only 2–5 cm away from the electron-beam path. The filament wires were moved greater than 10 cm away from the beam path and were also twisted together in order to reduce the strength of the magnetic field produced along the electron beam. By employing a dummy current load external to the vacuum system, 3 A was sent through the filament wires. With the vacuum system open to allow probe access, the magnetic field in the collision chamber was measured to be less than 2 mGauss for the new arrangement. Additionally, some magnetic components were removed from the electron-gun assembly and replaced with nonmagnetic materials.

During the previous measurements of the Ar I (106.7 nm) and Ar I (104.8 nm) lines, the heat sink that cools the electron-gun housing was not in good thermal contact with the water-cooling jacket. This led to elevated gas temperatures with greater uncertainties and caused larger errors in the oscillator strength measurements. Although this was discovered and remedied for the other measurements reported in Ref. [1], the Ar measurements were not redone until this work. The better temperature measurements in the present work allow us to report more precise oscillator strengths for the Ar resonance lines.

The reemission shield that surrounds the electron-atom source was significantly improved for the present work. The shield consists of a 1.5-cm i.d. hollow cylinder with a slit aligned with both the electron-atom source and the spectrometer entrance slit. The length of the slit was reduced by a factor of 3, thus requiring more careful alignment of the shield and spectrometer-detector system while providing sig-

nificantly improved reemission shielding. The cylindrical shield was also lengthened so that the exposed area of the electron-atom source that is not in line with the spectrometer was reduced. We estimate that the amount of stray radiation was reduced to less than 20% of its previous value.

The redesigned experimental apparatus was also tested for possible systematic effects due to the electron-gun settings. The electron beam is collimated by adjusting one main Einzel lens and observing the beam current impinging on floating collector plates along the beam path. Three other focusing lenses may also be used to fine tune the collimation. One transmission point for the He I (58.4 nm) transition was measured three times with a target gas pressure of about 14 μ Torr. The first measurement was taken with the optimum electron-beam-gun settings. For these optimum settings less than 0.25 μ A out of approximately 200 μ A of electron-beam current hit the exit aperture of the collision region. The second measurement had the secondary focusing adjustments varied in order to let up to 1 μ A hit the exit aperture of the collision region. The third transmission measurement had the primary and also the secondary lenses adjusted.

After the data were collected, the three results were scaled according to the theoretical transmission curve predicted by Schiff's oscillator strength in order to account for a 3% drift in target gas pressure which occurred during the set of three measurements. Measurements 1 and 2 were identical. Measurement 3 was slightly more than 1σ lower than measurements 1 and 2 but this is well within the statistical error for the two measurements. The conditions for measurement 3 were drastically different from 1 and 2. The changes in electron-gun settings were about an order of magnitude greater than would normally occur from drifting during a typical transmission scan. Electron-gun lens settings and drifts in electron-beam position have been eliminated as significant sources of systematic errors in the present experimental apparatus.

IV. DATA-COLLECTION PROCEDURE

The data are collected using a three-channel micro computer-controlled counting system which also records the measurement length and the time. After choosing an approximate pressure, the gas cell is allowed to equilibrate for 15–20 min while the target-gas pressure reaches a steady-state value. A measurement of $T_R(a_0x)$ at one gas density consists of recording the photon counts from the photomultiplier, the pressure counts from the ion gauge, and the electron-beam current counts from a digital multimeter. After these data are accumulated, an automatic valve is switched and the target gas is directed into the pumping system, rather than into the gas cell, and background measurements are performed. The cycle between target gas and background gas is repeated 3–15 times for each point on the transmission curve. Data are collected until the total number of signal minus background counts is around 15 000 or more. The transmission signal is taken to be the number of photon counts with the target gas in the cell minus the photon counts with only background gases in the cell normalized to both the pressure signal (target minus background) and the electron-beam current. Both the pressure and the electron-beam current are stable to better than 1% but this normaliza-

tion is necessary to achieve the transmission function precision desired.

V. ERROR ANALYSIS

The error analysis of these measurements has previously been discussed extensively [1]. One source of error that was not previously included in the analysis is the systematic error due to the reemission of the self-absorbed radiation. These measurements depend upon the absorption of resonant radiation which is then isotropically reemitted. Some fraction of this radiation will then make its way into the spectrometer-detector system. This leads to a systematic lowering of measured oscillator strengths since the more radiation that is absorbed and reemitted in this fashion, the greater the resulting photon counts due to reemitted light making its way into the detector. Since the spectrometer entrance slit covers such a small solid angle, it was previously believed that this fraction is very small with respect to the amount of radiation directly collected by the detection system. During the present study we were able to improve our understanding of this source of error.

As discussed above, the quantity of off-axis radiation escaping from the electron-atom source has been reduced by about a factor of 5. Therefore, a systematic error in our previous measurements should be revealed in a comparison of our old and new data. However, since we have modified other factors as well, the analysis is not so straightforward. A check was made on the He I (58.4 nm) line in order to test the sole effect of the present shielding. The measured oscillator strength was found to increase by about 1.5% when the emission baffle was improved. The random error in the fit parameter used to determine the oscillator strength is around 2% so this change is not statistically significant. This test does provide important information, though. Since a change of less than 2% was observed in the He I (58.4 nm) oscillator strength for a reduction of a factor of 5 in emitted light, we believe that 0.5% is an upper bound on the systematic error remaining due to the reemission of resonance radiation. Note that this effect is dependent on the resonance line under consideration and we only specifically investigated the He I (58.4 nm) line.

VI. RESULTS

A. Helium

The transmission function for the He I transition at 58.4 nm (2^1P_1) (circles) is shown in Fig. 1. The error bars shown include the uncertainties due to temperature fluctuations, counting statistics, changes in background pressure, and fluctuations in the electron-beam current and position. No systematic effects are included until the final analysis. These data were recorded with a target-gas temperature of 307 K and a spectrometer exit slit width of 0.07 mm. The oscillator strength determined from fitting the transmission function (solid line) to this data is 0.2700 ± 0.0076 (2.8%). The reduced χ^2 for this data set is 1.0. The transmission function for the He I transition at 53.7 nm (3^1P_1) (squares) is also shown in Fig. 1. These data were recorded with a gas temperature of 305 K and a spectrometer exit slit width of 0.07 mm. The measured oscillator strength is 0.0737 ± 0.0023

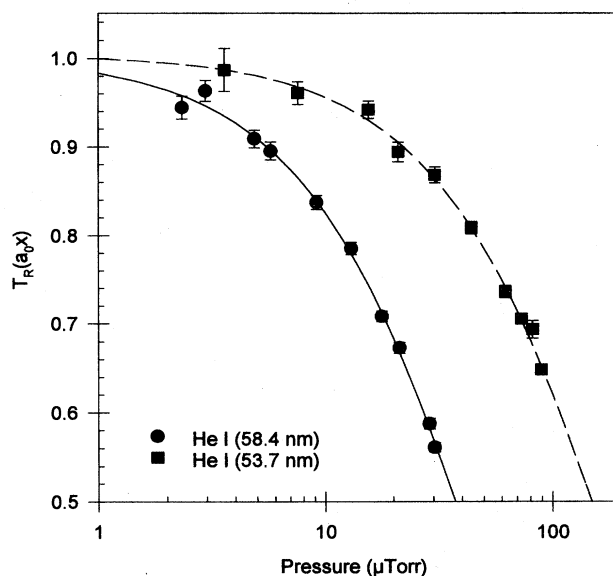


FIG. 1. Normalized transmission function versus He target-gas pressure in μTorr . The circles are the He I (58.4 nm) data points and the solid line is the fit to the data. The squares are the He I (53.7 nm) data points and the dashed line is the fit to the data.

(3.1%). The reduced χ^2 for this data set is 0.9 and the fitted transmission curve is shown as a dashed line.

Both of these He results are in excellent agreement with the theoretical values of Schiff [5]: He I (58.4 nm), 0.2762 ± 0.0001 ; He I (53.7 nm) 0.073 ± 0.001 . Schiff's theoretical results for He have been widely regarded as benchmark calculations. Two more recent sets of calculations are in excellent agreement with Schiff. The calculations of Cann and Thakkar [6] He I (58.4 nm), 0.27617 ± 0.00001 ; He I (53.7 nm) 0.07343 ± 0.00001 and those of Chen [7] He I (58.4 nm), 0.27611 ± 0.00001 ; He I (53.7 nm) 0.07342 ± 0.00001 are both within error of Schiff's results. The experimental result for the He I (58.4 nm) oscillator strength is 2.2% low compared to these theoretical results. The experimental result for the He I (53.7 nm) oscillator strength is 1.0% high compared to the calculated results. Both of these differences are less than 1σ .

The He I (58.4 nm) result is also in excellent agreement with the recent experimental result of Larsson *et al.* [8]. Larsson *et al.* obtained an oscillator strength of 0.269 ± 0.015 using two-color time-resolved spectroscopy to measure the mean lifetime. The present result is 0.37% higher than that of Larsson. The He I (53.7 nm) oscillator strength measurement is in excellent agreement with the experimental result of Astner *et al.* [9]. By using the theoretical branching fraction for this transition, Astner's high-precision beam-foil lifetime measurement has been converted to an oscillator strength of 0.073515 ± 0.00020 for comparison. The present result is 0.25% higher than that of Astner.

B. Neon

The transmission function for the Ne I transition at 74.4 nm ($2^2P_{3/2}$) (inverted triangles) is shown in Fig. 2. These data were recorded with a target-gas temperature of 329 K and a

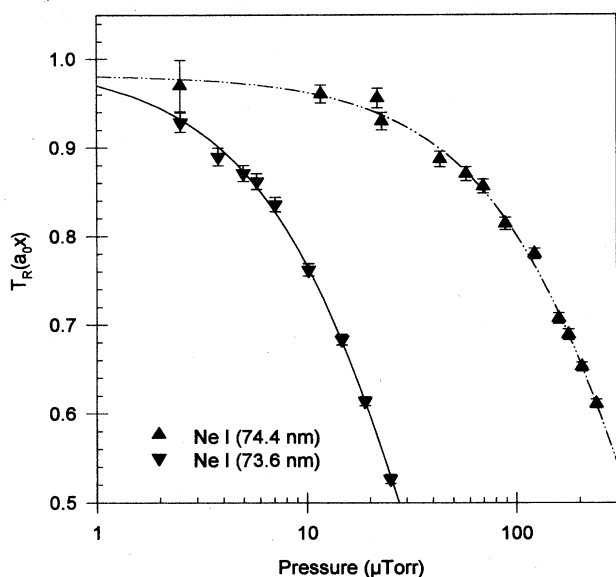


FIG. 2. Normalized transmission function versus Ar target-gas pressure in μTorr . The triangles are the Ar I (104.8 nm) data points and the dashed and dotted line is the fit to the data. The inverted triangles are the Ar I (106.7 nm) data points and the solid line is the fit to the data.

spectrometer exit slit width of 0.07 mm. The oscillator strength determined from fitting the transmission function (dashed line) to this data is 0.01095 ± 0.00032 (2.9%). The reduced χ^2 for this data set is 1.1. The transmission function for the Ne I transition at 73.6 nm ($^2P_{1/2}$) (triangles) is also shown in Fig. 2. These data were recorded with a gas temperature of 329 K and a spectrometer exit slit width of 0.07 mm. The measured oscillator strength is 0.1432 ± 0.0038 (2.6%). The transmission function is shown as a solid line and the reduced χ^2 for this data set is 0.6.

The present Ne results are in agreement with the intermediate coupling calculations of Aleksandrov *et al.* [10]: Ne I (74.4 nm), 0.0106; Ne I (73.6 nm), 0.141. These results are also in excellent agreement with the experimental results of Westerveld *et al.* [11]. Westerveld's results are Ne I (74.4 nm), 0.0109 ± 0.0009 ; Ne I (73.6 nm), 0.147 ± 0.012 .

C. Argon

The transmission function for the Ar I transition at 106.7 nm ($^2P_{3/2}$) (inverted triangles) is shown in Fig. 3. These data were recorded with a target-gas temperature of 305 K and a spectrometer exit slit width of 0.09 mm. The oscillator strength determined from fitting the transmission function (solid line) to this data is 0.0580 ± 0.0017 (2.9%). The reduced χ^2 for this data set is 0.7. The transmission function for the Ar I transition at 104.8 nm ($^2P_{1/2}$) (triangles) is also shown in Fig. 3. These data were recorded with a gas temperature of 305 K and a spectrometer exit slit width of 0.09 mm. The measured oscillator strength is 0.2214 ± 0.0068 (3.1%). The transmission function is shown as a dashed line and the reduced χ^2 for this data set is 0.9. Both Ar oscillator strengths are lower than our earlier results due to the previous temperature error and uncertainty.

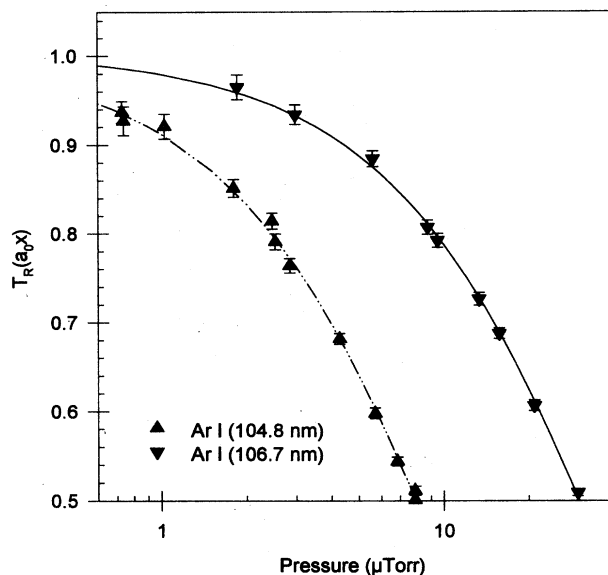


FIG. 3. Normalized transmission function versus Ne target-gas pressure in μTorr . The triangles are the Ne I (74.4 nm) data points and the dashed and dotted line is the fit to the data. The inverted triangles are the Ne I (73.6 nm) data points and the solid line is the fit to the data.

The present Ar results are in agreement with the many-configuration Hartree-Fock calculations of Gruzdev *et al.* [12]: Ar I (104.8 nm), 0.231 and Ar I (106.7 nm), 0.061. They are also in excellent agreement with the forward electron scattering experiments of Li *et al.* [13]: Ar I (104.8 nm), $0.22 + 0.02 - 0.03$, and Ar I (106.7 nm), $0.058 + 0.005 - 0.008$. The present Ar results are not in agreement with the recent

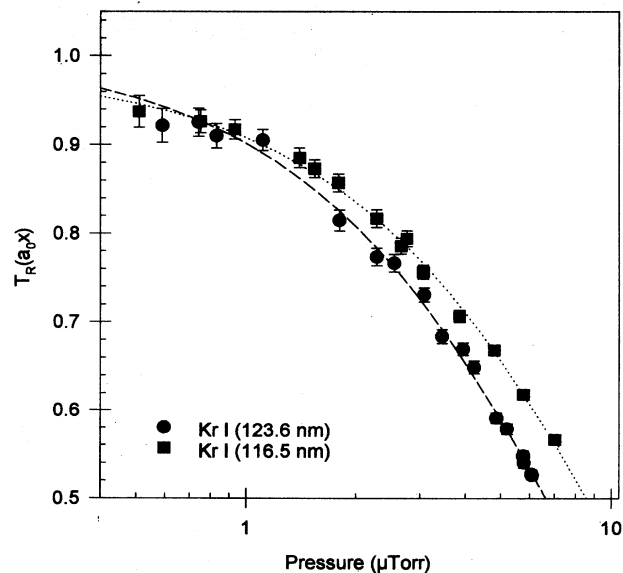


FIG. 4. Normalized transmission function versus target gas pressure in μTorr . The circles are the Kr I (123.6 nm) data points and the dashed line is the fit to the data. The squares are the Kr I (116.5 nm) data points and the dotted line is the fit to the data.

TABLE I. Oscillator strength results.

Line	OS	χ^2	% error (1σ)		Previous results Ref. [1]	% error (1σ)
He I (58.4 nm)	0.2700 ± 0.0076	1	2.8	+0.6	0.2683 ± 0.0075	2.8
He I (53.7 nm)	0.0737 ± 0.0023	0.9	3.1	+2.7	0.0717 ± 0.0024	3.4
Ne I (74.4 nm)	0.01095 ± 0.00032	1.1	2.9	+7.1	0.01017 ± 0.00030	2.9
Ne I (73.6 nm)	0.1432 ± 0.0038	0.6	2.6	+4.4	0.1369 ± 0.0035	2.6
Ar I (106.7 nm)	0.0580 ± 0.0017	0.7	2.9	-6.0	0.0616 ± 0.0021	3.4
Ar I (104.8 nm)	0.2214 ± 0.0068	0.9	3.1	-3.6	0.2297 ± 0.0093	4.0
Kr I (123.6 nm)	0.1775 ± 0.0050	0.1	2.8	+1.3	0.1751 ± 0.0049	2.8
Kr I (116.5 nm)	0.1416 ± 0.0041	0.8	2.9	-5.3	0.1496 ± 0.0038	2.5

beam-foil spectroscopy results of Federman *et al.* [14]. Federman measures the Ar I (104.8 nm) transition directly and finds an f value of 0.257 ± 0.013 (1σ). The f value of 0.064 ± 0.003 (1σ) for Ar I (106.7 nm) is obtained through a semi-empirical treatment of singlet-triplet mixing. Discussions with Federman did not reveal any explanation for the discrepancy. Nor are these results in agreement with the high-resolution dipole (e, e) measurements of Chan *et al.*: Ar I (106.7 nm), 0.0662 ± 0.0033 ; Ar I (104.8 nm), 0.265 ± 0.013 [15]. Since Federman's and Chan *et al.*'s results are recent, they were not included in Ref. [1] and are included here for completeness.

D. Krypton

The transmission function for the Kr I transition at 123.6 nm ($^2P_{3/2}$) (circles) is shown in Fig. 4. These data were recorded with a target-gas temperature of 331 K and a spectrometer exit slit width of 0.07 mm. The oscillator strength determined from fitting the transmission function (dashed line) to this data is 0.1175 ± 0.0050 (2.8%). The reduced χ^2 for this data set is 1.1. The transmission function for the Kr I transition at 116.5 nm ($^2P_{1/2}$) (squares) is also shown in Fig. 4. These data were recorded with a gas temperature of 331 K and a spectrometer exit slit width of 0.07 mm. The measured oscillator strength is 0.1416 ± 0.0041 (2.9%). The transmission function is shown as a dotted line and the reduced χ^2 for this data set is 0.8.

Krypton is such a complex atom that the theoretical results for the oscillator strengths vary widely, even for the first two resonance levels investigated here. With this in mind, a comparison will be made only to a set of experimental values. The absolute self-absorption work of Tsurubuchi *et al.* [16] produced results of Kr I (123.6 nm), 0.155 ± 0.011 and Kr I (116.5 nm), 0.139 ± 0.010 . The Kr I (123.6 nm) oscillator strength is in acceptable agreement and the Kr I (116.5 nm) oscillator strength is in excellent agreement with Tsurubuchi's result. Like the Ar self-absorption measurements,

the Kr results are also significantly lower than the high-resolution dipole (e, e) measurements of Chan *et al.*: Kr I (123.6 nm), 0.214 ± 0.011 and Kr I (116.5 nm), 0.193 ± 0.010 [13].

E. Summary

Table I is a summary of the oscillator strengths measured along with the error in each measurement. The quoted errors are the one sigma statistical plus systematic errors in each result. Also included are the reduced χ^2 for each fit to the transmission curve and the percentage change from our previous measurements as well as the previous values for the oscillator strengths. Table II gives the oscillator strength ratio for each pair of noble-gas resonance lines. These ratios allow useful comparisons to theoretical calculations. Since much of the error in the oscillator strength results is systematic, the percentage error in the ratios is much smaller than would be calculated by adding the individual errors in quadrature. The errors in the ratios include statistical errors from the transmission curve fits and the small systematic errors due to changes in transmission distance, temperature, and pressure. The errors in the ratios caused by systematic shifts in temperature, pressure and transmission distance are quite small since these shifts are in the same direction for both the numerator and the denominator. Therefore, the overall error is very close to the two statistical errors [from the fits to the transmission curves, $T_R(a_0x)$] added in quadrature. Also included in Table II are ratio values for comparison and the percentage difference between the present ratios and the values from the literature.

VII. DISCUSSION

After the previous series of oscillator strength measurements, our understanding of potential systematic errors was significantly improved. This increased understanding warranted a second generation of oscillator strength experiments

TABLE II. Oscillator strength ratios.

	Present ratio	% error (1σ)	Reference	$\Delta\%$
He 584:He 537	3.666 ± 0.102	2.8	3.784 ± 0.005 [5] theory	3.1
Ne 736:Ne 744	13.08 ± 0.31	2.4	13.30 ± 0.16 [9] theory	1.7
Ar 1067:Ar 1048	0.262 ± 0.005	1.9	0.264 ± 0.004 [6] theory	0.78
Kr 1236:Kr 1165	1.253 ± 0.031	2.5	1.12 ± 0.11 [11] experiment	-12.4%

employing the revised techniques and the modified apparatus described here. The newly measured oscillator strengths exhibit somewhat lower errors and a slight upward trend compared to the previous results with the similar apparatus. We believe this upward shift is the result of more complete re-emission shielding and the resulting decreased systematic error due to collection of reemitted resonant photons. The excellent values for χ^2 point to the fact that there is no significant reemission contribution since reemitted resonance radiation entering the spectrometer changes the shape of the transmission curve.

The two exceptions to this trend are the Ar oscillator strengths and the Kr 116.5-nm measurement. The present Ar experiments were conducted with a significantly improved gas temperature measurement. This effect applies only to the Ar data since the cooling system upgrades and temperature measurement improvements were instituted between the previous Ar measurements and the rest of the previous work. The older Kr 116.5-nm oscillator strength data had the largest deviation from our transmission theory ($\chi^2=1.6$). Potential explanations for the previous discrepancy are a possible

drift in temperature during the transmission measurement or a shift in the photon counting efficiency. The present measurement agrees well with the transmission theory ($\chi^2=0.8$) and therefore the authors believe the present measurements to be more valid.

In conclusion, measurements of eight noble-gas oscillator strengths have been performed. This work employed state-of-the-art pressure and temperature measurements to precisely determine the target-gas number density. The improved understanding and the resulting minimization of systematic errors helps make these absolute oscillator strengths some of the most precise self-absorption measurements to date.

ACKNOWLEDGMENTS

The authors wish to thank Rob Ligtenberg for his careful work on the experimental apparatus and Norbert Seifert, Mike Powers, and Steve Renwick for helpful discussions concerning this work. This work was supported in part by NSF Grant No. PHY90-16986.

-
- [1] R. C. G. Ligtenberg *et al.*, Phys. Rev. A **49**, 2363 (1994).
 [2] J. S. Risley and W. B. Westerveld, Appl. Opt. **28**, 389 (1989).
 [3] A. McPherson, N. Rouze, W. B. Westerveld, and J. S. Risley, Appl. Opt. **25**, 298 (1986).
 [4] R. C. G. Ligtenberg, Ph.D. thesis, North Carolina State University, 1992 (unpublished).
 [5] B. Schiff, C. L. Pekeris, and Y. Accad, Phys. Rev. A **4**, 885 (1971).
 [6] N. M. Cann and A. J. Thakkar, Phys. Rev. A **46**, 5397 (1992).
 [7] M. Chen, J. Phys. B **27**, 865 (1994).
 [8] J. Larsson, E. Mevel, R. Zerne, A. L'Huillier, C.-G. Wahlström, and S. Svanberg, J. Phys. B **28**, L53 (1995).
 [9] G. Astner, L. J. Curtis, L. Liljeby, S. Mannervik, and I. Martinson, Z. Phys. A **279**, 1 (1976).
 [10] Y. M. Aleksandrov, P. F. Gruzdev, M. G. Kozlov, A. V. Loginov, V. N. Makhov, R. V. Fedorchuk, and M. N. Yakimenko, Opt. Spektrosk. **54**, 4 (1983).
 [11] W. B. Westerveld, T. F. A. Mulder, and J. v. Eck, J. Quantum Spectrosc. Radiat. Transfer **21**, 533 (1979).
 [12] P. F. Gruzdev and A. V. Loginov, Opt. Spektrosk. **38**, 411 (1975).
 [13] G. P. Li, T. Takayanagi, K. Wakiya, H. Suzuki, T. Ajiro, S. Yagi, S. S. Kano, and H. Takuma, Phys. Rev. A **38**, 1240 (1988).
 [14] S. R. Federman, D. J. Beideck, and R. M. Schectman, Astrophys. J **401**, 367 (1992).
 [15] W. F. Chan, G. Cooper, X. Guo, G. R. Burton, and C. E. Brion, Phys. Rev. A **46**, 149 (1992).
 [16] S. Tsurubuchi, K. Wantanabe, and T. Arikawa, J. Phys. B **22**, 2969 (1989).